IEEE Access
Multidisciplinary ⋮ Rapid Review ⋮ Open Access Journal

Received 2 December 2023, accepted 15 December 2023, date of publication 22 December 2023,
date of current version 28 December 2023.

Digital Object Identifier 10.1109/ACCESS.2023.3346063

RESEARCH ARTICLE

Joint Identification for Number of Transmit Antennas and Channel Order

CHAO WANG[1], BOXIANG HE[2], AND FANGGANG WANG[2], (Senior Member, IEEE)
[1]China Academy of Space Technology, Beijing 100094, China
[2]State Key Laboratory of Advanced Rail Autonomous Operation, Frontiers Science Center for Smart High-Speed Railway System, School of Electronic and Information Engineering, Beijing Jiaotong University, Beijing 100044, China

Corresponding authors: Boxiang He (boxianghe1@bjtu.edu.cn) and Fanggang Wang (wangfg@bjtu.edu.cn)

This work was supported in part by the Fundamental Research Funds for the Central Universities under Grant 2022JBQY004, in part by the State Key Laboratory of Advanced Rail Autonomous Operation under Grant RCS2022ZT011, in part by the National Key Research and Development Program of China under Grant 2020YFB1806903, in part by the National Natural Science Foundation of China under Grant 62221001, and in part by the Joint Funds for Railway Fundamental Research of National Natural Science Foundation of China under Grant U2368201.

ABSTRACT Identifying the number of transmit antennas and the channel order is an important step in recovering the original information for a non-cooperative communication system. Traditional methods overestimate the number of transmit antennas and the channel order due to the coupling effect. This paper proposes a novel joint identification scheme to determine the number of transmit antennas and the channel order, which consists of two stages. Specifically, in the first stage, an improved weighted Gerschgorin disk identifier is developed to obtain the number of transmit antennas using frequency domain signals. In the second stage, we first derive an equivalent time-domain model to improve the utilization of the receiver antenna, and then a novel test statistic following F distribution is constructed to perform the sequential binary hypothesis testing. Finally, the channel order is obtained using the estimated number of transmit antennas in the first stage. The simulation results show that the proposed joint identification scheme significantly outperforms the existing approaches.

INDEX TERMS Antennas, additive white noise, cognitive radio, frequency division multiplexing, information security, multipath channels, receivers, signal detection, transmitters, wireless communication.

I. INTRODUCTION

Signal identification is a technology for identifying the unknown transmission parameters of a signal. Application areas include spectrum monitoring, cognitive radio, physical layer authentication, network security, and the industrial Internet of Things [1], [2], [3], [4], [5], [6], [7], [8]. With the rapid development of multiple-input multiple-output orthogonal frequency division multiplexing (MIMO-OFDM) systems in the last decade, signal identification in the transmission paradigm has attracted extensive attention because it can significantly reduce the pilot overhead by estimating the transmission parameters [9], [10], [11], [12], [13], [14], [15]. In this paper, we focus on the identification of the number of transmit antennas and the channel order in the MIMO-OFDM system, which are the essential steps for the subsequent information recovery. The existing work [16], [17], [18], [19], [20], [21], [22], [23], [24], [25], [26], [27], [28], [29], [30], [31] addresses these two issues separately, and thus cannot be employed for MIMO-OFDM systems with the multiple channel paths. This is mainly because the existing work is based on the fundamental assumptions that 1) the channel order is 1 for the identification of the number of transmit antennas, or 2) the number of transmit antennas is 1 for the identification of the channel order. Thus, when relaxing these assumptions, the identification of the number of transmit antennas and the channel order needs to be redesigned.

A. RELATED WORK

Identifying the number of transmit antennas can be regarded as an extension of source number detection in the array signal processing. For the identification of the number of transmit

The associate editor coordinating the review of this manuscript and approving it for publication was Gerard-Andre Capolino.

antennas, the existing literature [16], [17], [18], [19], [20], [21], [22], [23], [24] mainly falls into two classes: methods using the information theory criterion and those using the feature extraction. These methods require that the channel order is 1. In other words, the number of transmit antennas is overestimated with probability 1 for the MIMO-OFDM system with multiple channel paths. For methods using the information theory criterion, the number of transmit antennas is identified using the Akaike information criterion (AIC) and the minimum description length (MDL) [16]. Furthermore, the performance of the AIC and the MDL identifiers is evaluated for the spatially correlated MIMO system [17], which shows that the received spatial correlation does not affect the identification performance. However, both the AIC and the MDL identifiers have the following shortcomings: 1) they only work under the mild signal-to-noise ratio (SNR) conditions; 2) they are sensitive to the timing and frequency offsets; 3) when the channel order is greater than 1, the two identifiers overestimate the number of transmit antennas.

Compared with the information-theoretic methods, the feature-based algorithms [18], [19], [20], [21], [22], [23], [24] can identify the unknown number of transmit antennas with a lower complexity. Using the pilot signal, an identification method of the number of transmit antennas is proposed for the OFDM system, in which only one receive antenna is required for the receiver. Subsequently, an estimator based on the second- and fourth-order decision statistics is proposed to obtain the number of transmit antennas without the pilot signal, where the statistics are constructed using the feature of the time-varying block fading channels [19]. Considerable work focuses on the identification of the number of transmit antennas by using the sample covariance matrix. For example, in the earlier work [20], the one-step predicted eigenvalue threshold (PET) algorithm is proposed to estimate the number of signals by finding the upper threshold of the eigenvalues of the sample covariance matrix. Many hypothesis-testing-based algorithms are proposed to estimate the number of transmit antennas [21], [22], [23], which perform better under a wide range of SNR and sample lengths than the previous algorithms such as AIC, MDL, and PET. Recently, great progress has been made in identifying the number of transmit antennas based on the deep learning, which obtains the source number by formulating the source detection as a multi-class classification problem solved using deep learning frameworks. The normalized upper triangle of the autocorrelation matrix [24], the subspace-rank features [25], the eigenvalues of the normalized covariance matrix [26], the eigenvalue preprocessing [27], and the logarithmic eigenvalue [28] are extracted for the input features. The deep-learning-based methods can obtain a significant performance improvement compared to the methods based on non-deep-learning. However, all of the above methods overestimate the number of transmit antennas with a probability 1 when the channel order is greater than 1. In contrast to the existing methods, we propose an improved weighted Gerschgorin disk identifier to detect the number of transmit antennas using the frequency domain signal, which can combat the effect of multiple channel paths.

The channel order (or the number of the channel paths) is required to be obtained accurately before the channel estimation and equalization algorithms. Existing literature [29], [30], [31], [32], [33], [34], [35] focuses on the channel order identification of a single antenna transmitter. Thus, the existing methods often overestimate the channel order for multiple antenna transmitters. A generalized misspecified Cramer-Rao bound for the channel estimation under the channel order misspecification is introduced via the moore-penrose inverse operator [29]. Channel order identification is also a basic pattern analysis problem, which can be solved using the information theory criteria, such as the AIC and the MDL. However, the information-theory-criterion-based approaches often underestimate or overestimate the channel order. Various channel order identification methods have been proposed in the literature to obtain the channel order with the higher identification accuracy [30], [31], [32], [33], [34], [35]. For example, the subspace [30], [31], [32], the autocorrelation function [33], the hypothesis test [34], [35], and the cumulant features [36] are exploited to identify the unknown channel order. Despite a variety of schemes for the channel order identification, they can only operate in a single-antenna transmitter.

B. MAIN CONTRIBUTION

Because the existing methods handle the identification of the number of transmit antennas and the channel order separately, they suffer from serious overestimation problems in MIMO-OFDM systems with multiple channel paths. Different from the existing methods, we propose a novel joint identification scheme for the number of transmit antennas and the channel order in the MIMO-OFDM system, which well addresses the overestimation problem caused by the coupling of the multiple antennas and the multiple channel paths. Specifically, an improved weighted Gerschgorin disk identifier is proposed in the frequency domain, which introduces a diagonal matrix based on the second moment of the circle center and an adaptive threshold. Subsequently, the number of transmit antennas is coarsely identified in each subcarrier, and then the fine solution is determined by the max-win strategy over all subcarriers. Furthermore, we derive an equivalent time-domain model for the MIMO-OFDM system to improve the receive antenna utilization and construct a test statistic following the F distribution. Using the sequential binary hypothesis testing, the value of an expression containing the number of transmit antennas, the channel order, and the number of observations can be determined. As a consequence, the channel order can be detected using the identified number of transmit antennas in the frequency domain. The major contributions of our work are summarized as follows:

- Propose a joint identification scheme of the number of transmit antennas and the channel order for the MIMO-OFDM system. The proposed scheme can

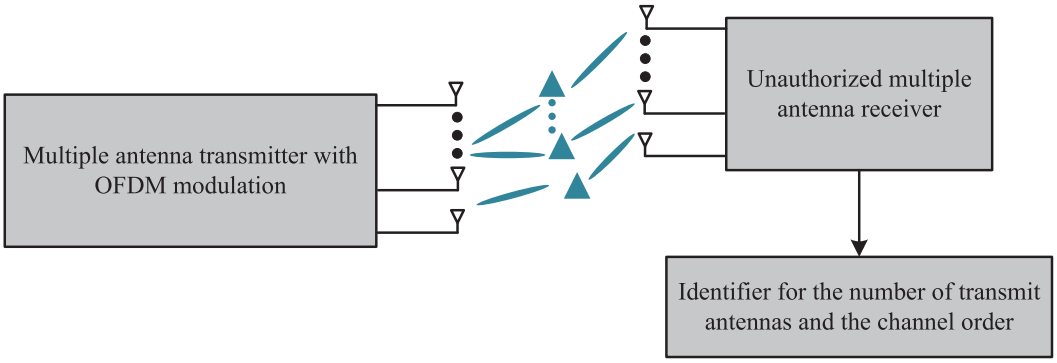

FIGURE 1. System model for the non-cooperative MIMO-OFDM communication with the multiple channel paths, where the multiple antenna transmitter sends the OFDM modulation signal and the unauthorized multiple antenna receiver determines the number of transmit antennas and the channel order using a well-designed identifier.

combat the coupling effect, and shows the excellent identification performance even at a very high SNR. In contrast, the traditional methods based on the information theory criteria or the subspace fail at a high SNR.

- Design an improved weighted Gerschgorin disk identifier to obtain the number of transmit antennas in the frequency domain, where the diagonal matrix based on the second moment of the circle center and an adaptive threshold are designed to accurately determine the position of the signal and error disks. The results show that the improved weighted Gerschgorin disk identifier outperforms the traditional approaches.
- Derive an equivalent time-domain model for the MIMO-OFDM system to improve the utilization of the receiver antenna. Furthermore, a novel test statistic following the F distribution is constructed to identify the channel order in the time domain by performing the sequential binary hypothesis testing. The proposed identifier is asymptotically consistent and has a higher identification accuracy than the existing methods.

The remainder of this paper is organized as follows. Section II introduces the system model. In Section III, we analyze the frequency model and propose an improved weighted Gerschgorin disk identifier. The equivalent time-domain model and the identifier based on F distribution are proposed in Section IV. In Section V, we analyze the performance of the proposed identifier. Section VI concludes this paper.

II. SYSTEM MODEL

In this section, the system model is first introduced. Then, we analyze the reasons why the number of transmit antennas and the channel order cannot be well identified in the MIMO-OFDM system.

Consider a non-cooperative MIMO-OFDM communication system, as shown in Fig. 1, where N_{t} transmit antennas and N_{r} receive antennas are employed in the transmitter and the unauthorized receiver, respectively. Assume that $N_{\mathrm{r}} > N_{\mathrm{t}}$. The received signal $\boldsymbol{y}(n) \in \mathbb{C}^{N_{\mathrm{r}}}$ at the unauthorized receiver is written by

$$\boldsymbol{y}(n) = \sum_{l=0}^{L-1} \boldsymbol{H}(l)\boldsymbol{x}(n-l) + \boldsymbol{w}(n), \quad n \in \mathcal{I}_N \tag{1}$$

where $\mathcal{I}_N = \{1, 2, \ldots, N\}$ denotes a shorthand of the index set; $\boldsymbol{x}(n) \in \mathbb{C}^{N_{\mathrm{t}}}$ is the transmitted nth signal sample; $\boldsymbol{H}(l) \in \mathbb{C}^{N_{\mathrm{r}} \times N_{\mathrm{t}}}$ is the lth channel fading matrix; L represents the channel order; N is the number of observed samples; $\boldsymbol{w}(n) \in \mathbb{C}^{N_{\mathrm{r}}}$ is the white noise, which follows the independent identically distributed (i.i.d) zero-mean circularly symmetric complex Gaussian (CSCG) distribution with the variance σ^2.

Let $\boldsymbol{H} = [\boldsymbol{H}(0), \boldsymbol{H}(1), \ldots, \boldsymbol{H}(L-1)]$ and $\tilde{\boldsymbol{x}}(n) = [\boldsymbol{x}^{\mathsf{T}}(n), \boldsymbol{x}^{\boldsymbol{T}}(n-1), \ldots, \boldsymbol{x}^{\mathsf{T}}(n-L+1)]^{\mathsf{T}}$, where T denotes the transpose. Then, the equation (1) can be further expressed as

$$\boldsymbol{y}(n) = \boldsymbol{H}\tilde{\boldsymbol{x}}(n) + \boldsymbol{w}(n), \quad n \in \mathcal{I}_N. \tag{2}$$

Furthermore, the statistical covariance matrix of the received signal is formulated by

$$\boldsymbol{\Gamma} = \mathbb{E}\left(\boldsymbol{y}(n)\boldsymbol{y}(n)^{\dagger}\right) \tag{3}$$

$$= \boldsymbol{H}\boldsymbol{R}_{\mathrm{x}}\boldsymbol{H}^{\dagger} + \sigma^2\boldsymbol{I}_{N_{\mathrm{r}}} \tag{4}$$

where $\boldsymbol{R}_{\mathrm{x}} = \mathbb{E}(\tilde{\boldsymbol{x}}(n)\tilde{\boldsymbol{x}}(n)^{\dagger})$ is the covariance matrix of the transmitted signal; $\mathbb{E}(\cdot)$ denotes the expectation with respect to all randomness; $\boldsymbol{I}_{N_{\mathrm{r}}}$ is the N_{r} by N_{r} identity matrix; $\dagger$ denotes the Hermitian transpose. Then, the eigenvalue decomposition (EVD) of the statistical covariance matrix $\boldsymbol{\Gamma}$ is expressed by

$$\boldsymbol{\Gamma} = \boldsymbol{U}\boldsymbol{\Lambda}\boldsymbol{U}^{\dagger} \tag{5}$$

where $\boldsymbol{U}$ is the unitary matrix formed by the eigenvectors of $\boldsymbol{\Gamma}$ and $\boldsymbol{\Lambda}$ denotes the diagonal matrix consisting of the eigenvalues of $\boldsymbol{\Gamma}$. Then, the ith eigenvalue λ_i of $\boldsymbol{\Gamma}$ satisfies

$$\begin{cases} \lambda_1 \geq \lambda_2 \cdots \geq \lambda_{N_{\mathrm{t}}L+1} = \cdots = \lambda_{N_{\mathrm{r}}} = \sigma^2, & N_{\mathrm{r}} > N_{\mathrm{t}}L \\ \lambda_1 \geq \lambda_2 \cdots \geq \lambda_{N_{\mathrm{r}}}, & \text{otherwise.} \end{cases} \tag{6}$$

We can see from (6) that $N_{\mathrm{t}}L$ can be estimated from the cardinality of the largest eigenvalues of $\boldsymbol{\Gamma}$ when $N_{\mathrm{r}} > N_{\mathrm{t}}L$ is

satisfied. However, in practice, we can only obtain the sample covariance matrix with finite sample sizes N, i.e.

$$\boldsymbol{\Gamma}_{\mathrm{s}} = \frac{1}{N}\sum_{n=1}^{N}\boldsymbol{y}(n)\boldsymbol{y}(n)^{\dagger}. \tag{7}$$

Thus, the ith eigenvalue λ_i^{s} of $\boldsymbol{\Gamma}_{\mathrm{s}}$ satisfies

$$\begin{cases} \lambda_1^{\mathrm{s}} \geq \lambda_2^{\mathrm{s}} \cdots \geq \lambda_{N_{\mathrm{t}}L+1}^{\mathrm{s}} \geq \cdots \geq \lambda_{N_{\mathrm{r}}}^{\mathrm{s}}, & N_{\mathrm{r}} > N_{\mathrm{t}}L \\ \lambda_1^{\mathrm{s}} \geq \lambda_2^{\mathrm{s}} \cdots \geq \lambda_{N_{\mathrm{r}}}^{\mathrm{s}}, & \text{otherwise.} \end{cases} \tag{8}$$

It can be observed from (8) that $N_{\mathrm{t}}L$ cannot be determined from the cardinality of the largest eigenvalues of $\boldsymbol{\Gamma}_{\mathrm{s}}$ even when $N_{\mathrm{r}} > N_{\mathrm{t}}L$ is satisfied. This is because the smallest $N_{\mathrm{r}} - N_{\mathrm{t}}L$ eigenvalues in (8) are different. In fact, the existing methods such as the AIC, the MDL, and the PET methods provide a solution for the estimation of $N_{\mathrm{t}}L$ when $N_{\mathrm{r}} > N_{\mathrm{t}}L$ is satisfied. However, the previous work cannot determine the number of transmit antennas N_{t} and the channel order L, respectively. In our work, the goal is to determine the number of transmit antennas and the channel order simultaneously with finite sample sizes only when $N_{\mathrm{r}} > N_{\mathrm{t}}$ is satisfied.

III. FREQUENCY DOMAIN MODEL AND IMPROVED WEIGHTED GERSCHGORIN DISK IDENTIFIER

In this section, we first extend the time domain model of the MIMO-OFDM system to the frequency domain. Then, the Gerschgorin disk theorem is introduced. Furthermore, the number of transmit antennas in each subcarrier is identified by the improved weighted Gerschgorin disk identifier, which introduces a diagonal matrix based on the second moment of the circle center and an adaptive threshold. Finally, the number of transmit antennas is determined using the max-win strategy over all subcarriers.

A. FREQUENCY DOMAIN MODEL

Assume that a block has M OFDM symbols and the number of the subcarrier is P. Let $\boldsymbol{X}(p,m) = [X_1(p,m), X_2(p,m), \ldots, X_{N_{\mathrm{t}}}(p,m)]^{\mathsf{T}}$ denote the mth transmitted symbol of the pth subcarrier, where $m \in \mathcal{I}_M$ and $p \in \mathcal{I}_P$. For the pth subcarrier, the transmitted signal with M symbols can be expressed by

$$\boldsymbol{X}_p = [\boldsymbol{X}(p,1), \boldsymbol{X}(p,2), \ldots, \boldsymbol{X}(p,M)] \tag{9}$$

$$= \begin{bmatrix} X_1(p,1) & X_1(p,2) & \cdots & X_1(p,M) \\ X_2(p,1) & X_2(p,2) & \cdots & X_2(p,M) \\ \vdots & \vdots & \ddots & \vdots \\ X_{N_{\mathrm{t}}}(p,1) & X_{N_{\mathrm{t}}}(p,2) & \cdots & X_{N_{\mathrm{t}}}(p,M) \end{bmatrix}. \tag{10}$$

Let $\boldsymbol{Y}(p,m) = [Y_1(p,m), Y_2(p,m), \ldots, Y_{N_{\mathrm{r}}}(p,m)]^{\mathsf{T}}$ be the mth received symbol of the pth subcarrier. The received signal in the frequency domain can be denoted by

$$\boldsymbol{Y}_p = [\boldsymbol{Y}(p,1), \boldsymbol{Y}(p,2), \ldots, \boldsymbol{Y}(p,M)] \tag{11}$$

$$= \begin{bmatrix} Y_1(p,1) & Y_1(p,2) & \cdots & Y_1(p,M) \\ Y_2(p,1) & Y_2(p,2) & \cdots & Y_2(p,M) \\ \vdots & \vdots & \ddots & \vdots \\ Y_{N_{\mathrm{r}}}(p,1) & Y_{N_{\mathrm{r}}}(p,2) & \cdots & Y_{N_{\mathrm{r}}}(p,M) \end{bmatrix}. \tag{12}$$

The channel frequency response of the pth subcarrier is formulated as

$$\boldsymbol{H}_p = \begin{bmatrix} H_{1,1}(p) & H_{1,2}(p) & \cdots & H_{1,N_{\mathrm{t}}}(p) \\ H_{2,1}(p) & H_{2,2}(p) & \cdots & H_{2,N_{\mathrm{t}}}(p) \\ \vdots & \vdots & \ddots & \vdots \\ H_{N_{\mathrm{r}},1}(p) & H_{N_{\mathrm{r}},2}(p) & \cdots & H_{N_{\mathrm{r}},N_{\mathrm{t}}}(p) \end{bmatrix} \tag{13}$$

where

$$H_{i,j}(p) = \sum_{l=0}^{L-1} h_l^{[i,j]} e^{-j2\pi\frac{pl}{P}}, \quad i \in \mathcal{I}_{N_{\mathrm{r}}},\ j \in \mathcal{I}_{N_{\mathrm{t}}} \tag{14}$$

where $h_l^{[i,j]}$ denotes the power gain of the lth path between the ith receive antenna and the jth transmit antenna. The frequency domain model is written by

$$\boldsymbol{Y}_p = \boldsymbol{H}_p\boldsymbol{X}_p + \boldsymbol{w}_p, \quad p \in \mathcal{I}_P \tag{15}$$

where $\boldsymbol{w}_p$ is the white noise, which follows i.i.d zero-mean CSCG distribution with the variance σ_p^2. Thus, the sample covariance matrix in the pth subcarrier can be formulated by

$$\boldsymbol{\Gamma}_{\mathrm{s}}^{[p]} = \frac{1}{M}\sum_{m=1}^{M}\boldsymbol{Y}_p\boldsymbol{Y}_p^{\dagger}, \quad p \in \mathcal{I}_P. \tag{16}$$

The statistical covariance matrix is approximated by computing the average of the sample covariance matrices with $M \to \infty$, i.e.

$$\boldsymbol{\Gamma}_p = \lim_{M\to\infty}\boldsymbol{\Gamma}_{\mathrm{s}}^{[p]} \tag{17}$$

$$= \lim_{M\to\infty}\frac{1}{M}\sum_{m=1}^{M}\boldsymbol{Y}_p\boldsymbol{Y}_p^{\dagger}, \quad p \in \mathcal{I}_P. \tag{18}$$

Then, we can obtain the equation (19) using EVD, i.e.

$$\boldsymbol{\Gamma}_p = \boldsymbol{U}_p\boldsymbol{\Lambda}_p\boldsymbol{U}_p^{\dagger}, \quad p \in \mathcal{I}_P \tag{19}$$

where $\boldsymbol{U}_p$ is the unitary matrix with $N_{\mathrm{r}} \times N_{\mathrm{r}}$ dimensions and

$$\boldsymbol{\Lambda}_p = \begin{cases} \sigma_p^2\boldsymbol{I}_{N_{\mathrm{r}}} + \mathrm{diag}\big(\lambda(p,1), \ldots, \lambda(p,N_{\mathrm{t}}), \varepsilon(p,N_{\mathrm{t}}+1), \\ \ldots, \varepsilon(p,N_{\mathrm{t}}L), 0_{N_{\mathrm{t}}L+1} \ldots, 0_{N_{\mathrm{r}}}\big), & N_{\mathrm{r}} > N_{\mathrm{t}}L, \\ \sigma_p^2\boldsymbol{I}_{N_{\mathrm{r}}} + \mathrm{diag}\big(\lambda(p,1), \ldots, \lambda(p,N_{\mathrm{t}}), \varepsilon(p,N_{\mathrm{t}}+1), \\ \ldots, \varepsilon(p,N_{\mathrm{r}})\big), & \text{otherwise} \end{cases} \tag{20}$$

where ε represents the error term caused by the multiple channel paths. Even if $M \to \infty$ is satisfied, the noise subspace is difficult to determine because of the error term. Thus, the traditional methods such as the AIC, the MDL, and the PET overestimate the number of transmit antennas. Specifically, the traditional methods are still effective at a low SNR but the performance is degraded. While at a high SNR, the traditional methods fail. This is because the higher

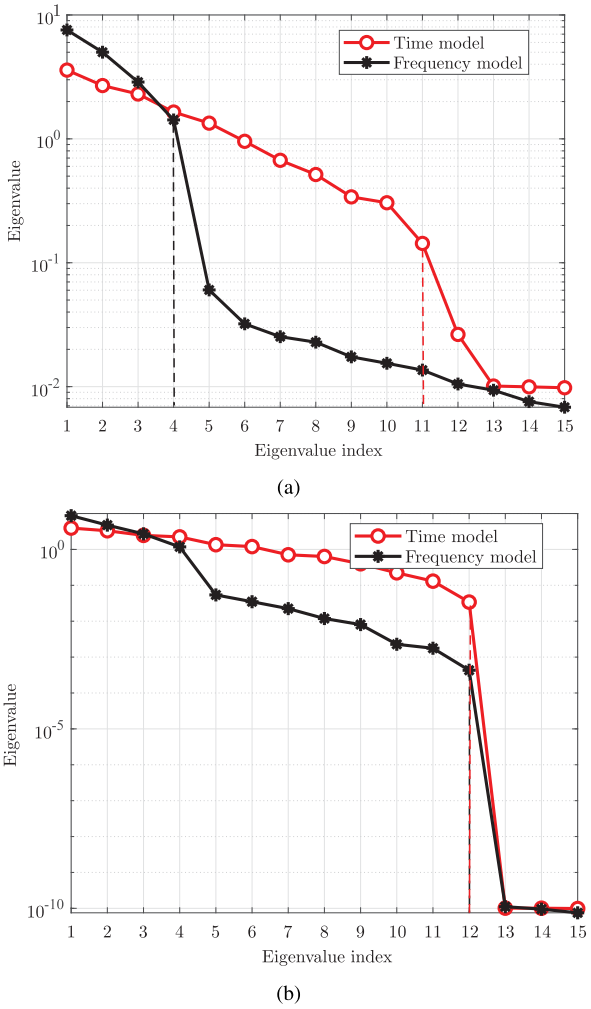

FIGURE 2. Eigenvalues of the sample covariance matrix for the time model and the frequency model in different signal-to-noise ratio conditions: (a) signal-to-noise ratio with 5 dB, and (b) signal-to-noise ratio with 20 dB.

the SNR, the greater the difference between the error term and the noise power. Fig. 2 shows that the eigenvalues of the sample covariance matrix in the time domain and the frequency domain models for $N_{\mathrm{t}} = 4$, $N_{\mathrm{r}} = 15$, and $L = 3$. We can see that, when the SNR is 5 dB, whether the time domain model or the frequency domain model is used, the eigenvalue of the sample covariance matrix only has an obvious jumping point. Furthermore, the value of $N_{\mathrm{t}}L$ can be obtained in the time domain model, and the value of N_{t} can be accurately obtained in the frequency domain model by using the traditional methods. As a comparison, when the SNR is 20 dB, there is only one step point in the time domain model, and the value of $N_{\mathrm{t}}L$ can be obtained through the step point. There are two jumping points in the frequency domain model and the jumping point in the index 12 is more obvious, so the traditional methods will overestimate the value of N_{t} as $N_{\mathrm{t}}L$. In the following, we theoretically consider how to determine the value of N_{t} using the covariance matrix $\boldsymbol{\Gamma}_p$ over all subcarriers only when $N_{\mathrm{r}} > N_{\mathrm{t}}$ is satisfied.

B. GERSCHGORIN DISK THEOREM

Gerschgorin disk theorem is often used to determine the locations of eigenvalues from the matrix $\boldsymbol{E}$ with $Q \times Q$ dimensions. Let

$$g_i = \sum_{j=1, j\neq i}^{Q} |e_{i,j}|, \quad i \in \mathcal{I}_Q \tag{21}$$

where $e_{i,j}$ is the element at the ith row and the jth column of the matrix $\boldsymbol{E}$. Then, the ith disk O_i is defined as the collection of points in the complex plane whose distance to $e_{i,i}$ is at most g_i, i.e.

$$O_i = \{z \in \mathbb{C} : |z - e_{i,i}| \leq g_i\} \tag{22}$$

where $e_{i,i}$ and g_i are the Gerschgorin center and the Gerschgorin radius, respectively. In [37], the authors proved that the eigenvalues of matrix $\boldsymbol{E}$ are contained in the union of disks O_i, $i \in \mathcal{I}_Q$.

C. IMPROVED WEIGHTED GERSCHGORIN DISK IDENTIFIER

In this section, we propose an improved weighted Gerschgorin disk identifier to determine the number of transmit antennas, where a diagonal matrix based on the second moment of the circle center and an adaptive threshold are carefully designed. The weighted Gerschgorin disk identifier increases the discrimination of the signal, error, and noise disks by the similarity transformation of the designed diagonal matrix. Furthermore, we construct an adaptive threshold based on the circle center to determine the value of N_{t}. The decision strategy based on the adaptive threshold is as follows: The decision starts with the signal disks and is stopped once the step is found. Finally, we determine the number of transmit antennas over all subcarriers using the max-win strategy, i.e., the value of N_{t} with the maximum number of votes is chosen as the decision.

The block representation of the matrix $\boldsymbol{\Gamma}_p$ in the equation (17) can be formulated by

$$\boldsymbol{\Gamma}_p = \begin{bmatrix} r_{1,1}(p) & r_{1,2}(p) & \cdots & r_{1,N_{\mathrm{r}}}(p) \\ r_{2,1}(p) & r_{2,2}(p) & \cdots & r_{2,N_{\mathrm{r}}}(p) \\ \vdots & \vdots & \ddots & \vdots \\ r_{N_{\mathrm{r}},1}(p) & r_{N_{\mathrm{r}},2}(p) & \cdots & r_{N_{\mathrm{r}},N_{\mathrm{r}}}(p) \end{bmatrix} \tag{23}$$

$$= \begin{bmatrix} \tilde{\boldsymbol{\Gamma}}_p & \boldsymbol{r} \\ \boldsymbol{r}^{\dagger} & r_{N_{\mathrm{r}},N_{\mathrm{r}}}(p) \end{bmatrix}, \quad p \in \mathcal{I}_P \tag{24}$$

where $\tilde{\boldsymbol{\Gamma}}_p$ is a matrix of the first $N_{\mathrm{r}} - 1$ rows and the first $N_{\mathrm{r}} - 1$ columns of $\boldsymbol{\Gamma}_p$, and $\boldsymbol{r}$ is the column vector formed by the first $N_{\mathrm{r}} - 1$ rows of the N_{r}th column in the matrix $\boldsymbol{\Gamma}_p$. Then, we can obtain the equation (25) using the EVD of $\tilde{\boldsymbol{\Gamma}}_p$, i.e.

$$\tilde{\boldsymbol{\Gamma}}_p = \tilde{\boldsymbol{U}}_p \tilde{\boldsymbol{\Lambda}}_p \tilde{\boldsymbol{U}}_p^{\dagger}, \quad p \in \mathcal{I}_P \tag{25}$$

where $\tilde{\boldsymbol{U}}_p = [\tilde{\boldsymbol{u}}_{p,1}, \tilde{\boldsymbol{u}}_{p,2}, \ldots, \tilde{\boldsymbol{u}}_{p,N_{\mathrm{r}}-1}]$ denotes the unitary matrix with $(N_{\mathrm{r}} - 1) \times (N_{\mathrm{r}} - 1)$ dimensions and $\tilde{\boldsymbol{\Lambda}}_p = \mathrm{diag}(\gamma_1, \gamma_2, \ldots, \gamma_{N_{\mathrm{r}}-1})$ is the diagonal matrix consisting of

the eigenvalues of $\tilde{\boldsymbol{\Gamma}}_p$ and $\gamma_1 > \gamma_2 > \cdots > \gamma_{N_\mathrm{r}-1}$. Let

$$\boldsymbol{U}'_p = \begin{bmatrix} \tilde{\boldsymbol{U}}_p & \boldsymbol{0} \\ \boldsymbol{0} & 1 \end{bmatrix}, \quad p \in \mathcal{I}_P. \tag{26}$$

Then, we transform the matrix $\boldsymbol{\Gamma}_p$ to $\boldsymbol{\Gamma}'_p$, i.e.

$$\begin{aligned} \boldsymbol{\Gamma}'_p &= (\boldsymbol{U}'_p)^\dagger \boldsymbol{\Gamma}_p \boldsymbol{U}'_p & (27)\\ &= \begin{bmatrix} \tilde{\boldsymbol{U}}_p^\dagger \tilde{\boldsymbol{\Gamma}}_p \tilde{\boldsymbol{U}}_p & \tilde{\boldsymbol{U}}_p^\dagger \boldsymbol{r} \\ \boldsymbol{r}^\dagger \tilde{\boldsymbol{U}}_p & r_{N_\mathrm{r},N_\mathrm{r}}(p) \end{bmatrix} & (28)\\ &= \begin{bmatrix} \gamma_1 & 0 & \cdots & 0 & \rho_1 \\ 0 & \gamma_2 & \ddots & \vdots & \rho_2 \\ \vdots & \ddots & \ddots & 0 & \vdots \\ 0 & \cdots & 0 & \gamma_{N_\mathrm{r}-1} & \rho_{N_\mathrm{r}-1} \\ \rho_1^* & \rho_2^* & \cdots & \rho_{N_\mathrm{r}-1}^* & r_{N_\mathrm{r},N_\mathrm{r}}(p) \end{bmatrix}, \quad p \in \mathcal{I}_P & (29) \end{aligned}$$

where $*$ denotes conjugate. Assume that $L = 1$, then, $\rho_i = 0$ when $i = N_\mathrm{t}+1, N_\mathrm{t}+2, \ldots, N_\mathrm{r}-1$, while $\rho_i \neq 0$, when $i = 1, 2, \ldots, N_\mathrm{t}$. This is because the noise eigenvectors $\tilde{\boldsymbol{u}}_{p,i}$, $i = N_\mathrm{t}+1, N_\mathrm{t}+2, \ldots, N_\mathrm{r}-1$ are orthogonal to the vector $\boldsymbol{r}$ and the signal eigenvectors $\tilde{\boldsymbol{u}}_{p,i}$, $i = 1, 2, \ldots, N_\mathrm{t}$ are non-orthogonal to the vector $\boldsymbol{r}$. Because the unitary transformation of the covariance matrix does not change the eigenvalues of $\boldsymbol{\Gamma}_p$, according to this Cauchy-poincar theorem, we can obtain

$$\begin{aligned} &\sigma_p^2 + \lambda(p,1) \geq \gamma_1 \geq \sigma_p^2 + \lambda(p,2) \geq \gamma_2 \geq \cdots \geq \\ &\quad \sigma_p^2 + \lambda(p,N_\mathrm{t}) \geq \gamma_{N_\mathrm{t}} \geq \sigma_p^2 = \gamma_{N_\mathrm{t}+1} = \cdots = \gamma_{N_\mathrm{r}-1}. \end{aligned} \tag{30}$$

From the Gerschgorin disk theorem, $|\rho_i|$ and γ_i are the radius and the circle center of the first $N_\mathrm{r}-1$ Gerschgorin disks of matrix $\boldsymbol{\Gamma}'_p$, respectively. Thus, the signal collection with larger Gerschgorin radii contains exactly N_t largest signal eigenvalues, and the noise collection with the smaller Gerschgorin radii contains the remaining noise eigenvalues. Furthermore, we can determine the number of transmit antennas by counting the number of non-zero radii. However, under the multiple channel paths, i.e, $L > 1$, the collection of the radius of the Gerschgorin disks is

$$\begin{cases} \{\overbrace{\rho_1, \ldots, \rho_{N_\mathrm{t}}}^{\text{The signal disks}}, \overbrace{\varepsilon'_{N_\mathrm{t}+1}, \ldots, \varepsilon'_{N_\mathrm{t}L}}^{\text{The error disks}}, \overbrace{0_{N_\mathrm{t}L+1}, \ldots, 0_{N_\mathrm{r}-1}}^{\text{The noise disks}}\}, & N_\mathrm{r} > N_\mathrm{t}L, \\ \{\overbrace{\rho_1, \ldots, \rho_{N_\mathrm{t}}}^{\text{The signal disks}}, \overbrace{\varepsilon'_{N_\mathrm{t}+1}, \ldots, \varepsilon'_{N_\mathrm{r}-1}}^{\text{The error disks}}\}, & \text{otherwise} \end{cases} \tag{31}$$

where ε' denotes the error term caused by the multiple channel paths. Here, we design a diagonal matrix based on the second moment of the circle center. The diagonal matrix, namely, the weighted matrix, is represented by

$$\boldsymbol{\Psi} = \begin{bmatrix} \boldsymbol{\Psi}_1 & \boldsymbol{0} \\ \boldsymbol{0} & \psi \end{bmatrix} \tag{32}$$

Algorithm 1 Improved Weighted Gerschgorin Disk Identifier

Input: Received signal $\boldsymbol{y}$;

1: Compute $\boldsymbol{\Gamma}_\mathrm{s}^{[p]}$ using (16);
2: Calculate $\boldsymbol{\Gamma}'_p$ using (27);
3: Compute $\boldsymbol{\Gamma}''_p$ using (33);
4: Construct the adaptive threshold $\varrho(k)$ using (35);
5: Obtain the collection $\{N_t^1, N_t^2, \ldots, N_t^P\}$;
6: Choose the value with maximum votes as the number of transmit antennas.

where $\boldsymbol{\Psi}_1 = \mathrm{diag}(\gamma_1^2, \gamma_2^2, \ldots, \gamma_{N_\mathrm{r}-1}^2)$, $\psi = \sum_{i=1}^{N_\mathrm{r}-1} \gamma_i^2$. Then, the similarity transform of $\boldsymbol{\Gamma}'_p$ is performed using the weighted matrix $\boldsymbol{\Psi}$, i.e.

$$\begin{aligned} \boldsymbol{\Gamma}''_p &= \boldsymbol{\Psi} \boldsymbol{\Gamma}'_p \boldsymbol{\Psi}^{-1} & (33)\\ &= \begin{bmatrix} \gamma_1 & 0 & \cdots & 0 & \frac{\gamma_1^2}{\psi}\rho_1 \\ 0 & \gamma_2 & \ddots & \vdots & \frac{\gamma_2^2}{\psi}\rho_2 \\ \vdots & \ddots & \ddots & 0 & \vdots \\ 0 & \cdots & 0 & \gamma_{N_\mathrm{r}-1} & \frac{\gamma_{N_\mathrm{r}-1}^2}{\psi}\rho_{N_\mathrm{r}-1} \\ \frac{\psi}{\gamma_1^2}\rho_1^* & \frac{\psi}{\gamma_2^2}\rho_2^* & \cdots & \frac{\psi}{\gamma_{N_\mathrm{r}-1}^2}\rho_{N_\mathrm{r}-1}^* & r_{N_\mathrm{r},N_\mathrm{r}}(p) \end{bmatrix}. & (34) \end{aligned}$$

Because $\psi = \sum_{i=1}^{N_\mathrm{r}-1} \gamma_i^2$, $\frac{\gamma_i^2}{\psi} < 1$. Furthermore, $\gamma_1 > \gamma_2 > \cdots > \gamma_{N_\mathrm{r}-1}$ holds, thus the discrimination among the signal disks, error, and noise disks increases by the similarity transform according to the equation (33). Next, we construct an adaptive threshold based on the circle center without the artificial adjustment. The adaptive threshold is expressed by

$$\varrho(k) = \rho'(k) - \frac{\gamma_{k+1}^2}{\sum_{i=1}^{N_\mathrm{r}-1}\gamma_i} \sum_{i=1}^{N_\mathrm{r}-1} \frac{\rho'(i)}{N_\mathrm{r}-1}, \quad k \in \mathcal{I}_{N_\mathrm{r}-2} \tag{35}$$

where $\rho'(k) = \frac{\gamma_k^2}{\psi}\rho_k$ denotes the radius of the transformed Gerschgorin disks, and the decision starts with the signal disks and is stopped once the step is found, i.e., $\varrho(k) < 0$. Then, the value of the number of transmit antennas in the pth subcarrier $N_\mathrm{t}^p = k - 1$. Finally, we determine the number of transmit antennas over all subcarriers using the max-win strategy, i.e., the value of $\hat{N}_\mathrm{t}$ with the maximum number of votes is chosen as the decision. The improved weighted Gerschgorin disk identifier is summarized in Algorithm 1.

IV. EQUIVALENT TIME-DOMAIN MODEL AND IDENTIFIER VIA *F* DISTRIBUTION

In this section, we first derive an equivalent time-domain model for the MIMO-OFDM system to improve the utilization of the receiver antenna. Then, we propose an identifier based on F distribution. Finally, we prove the asymptotic consistency of the proposed identifier.

A. EQUIVALENT TIME-DOMAIN MODEL

Consider K successive samples of the received signal sequence in the jth receive antenna, then the channel matrix

from the ith transmit antenna to the jth receive antenna with $K \times (K+L-1)$ can be formulated by

$$\boldsymbol{H}_{i,j} = \begin{bmatrix} h_{i,j}(0) & \cdots & h_{i,j}(L-1) & \\ & \ddots & & \ddots \\ & & h_{i,j}(0) & \cdots\ h_{i,j}(L-1) \end{bmatrix}. \quad (36)$$

Thus, the channel matrix can be expressed by

$$\bar{\boldsymbol{H}} = [\boldsymbol{H}_1^{\mathsf{T}}, \boldsymbol{H}_2^{\mathsf{T}}, \ldots, \boldsymbol{H}_{N_\mathrm{r}}^{\mathsf{T}}]^{\mathsf{T}} \quad (37)$$

where $\boldsymbol{H}_j = [\boldsymbol{H}_{1,j}, \boldsymbol{H}_{2,j}, \ldots, \boldsymbol{H}_{N_\mathrm{t},j}]$. Let $\boldsymbol{y}_K(n) = [y_1(n), \ldots, y_1(n-K+1), y_2(n), \ldots, y_2(n-K+1), \ldots, y_{N_\mathrm{r}}(n), \ldots, y_{N_\mathrm{r}}(n-K+1)]^{\mathsf{T}}$, $n \in \mathcal{I}_{N_\mathrm{s}}$, which is constructed by stacking K successive samples of the received signal sequence over all N_r receive antennas. Then, the equivalent time-domain model for the MIMO-OFDM system can be represented as

$$\boldsymbol{y}_K(n) = \bar{\boldsymbol{H}}\boldsymbol{x}_K(n) + \boldsymbol{v}(n), \quad n \in \mathcal{I}_{N_\mathrm{s}} \quad (38)$$

where $\boldsymbol{x}_K(n) = [x_1(n), \ldots, x_1(n-K-L+1), x_2(n), \ldots, x_2(n-K-L+1), \ldots, x_{N_\mathrm{t}}(n), \ldots, x_{N_\mathrm{t}}(n-K-L+1)]^{\mathsf{T}}$, and $\boldsymbol{v}(n)$ is the white noise following i.i.d zero-mean CSCG distribution with the variance σ^2. Thus, the statistical covariance matrix of $\boldsymbol{y}_K$ can be expressed by

$$\boldsymbol{\Omega} = \lim_{N_\mathrm{s}\to\infty} \frac{1}{N_\mathrm{s}} \sum_{n=1}^{N_\mathrm{s}} \boldsymbol{y}_K(n)\boldsymbol{y}_K(n)^\dagger. \quad (39)$$

As discussed in Section II, the eigenvalues of $\boldsymbol{\Omega}$ are first obtained by EVD, and then the value of $N_\mathrm{t}(K+L-1)$ can be determined by the cardinality of the largest eigenvalues of $\boldsymbol{\Omega}$ if $N_\mathrm{r}K > N_\mathrm{t}(K+L-1)$ is satisfied, i.e.

$$K > \frac{N_\mathrm{t}(L-1)}{N_\mathrm{r} - N_\mathrm{t}}. \quad (40)$$

The inequality (40) implies $N_\mathrm{t}(K+L-1)$ can be estimated theoretically with $N_\mathrm{r} > N_\mathrm{t}$ instead of $N_\mathrm{r} > N_\mathrm{t}L$.

B. IDENTIFIER VIA F DISTRIBUTION

Next, the goal is to determine the value of L. We propose a hypothesis-testing-based identifier, which obtains a high identification accuracy even at a low SNR. The eigenvector space of $\boldsymbol{\Omega}$ is formulated as

$$\begin{aligned} \boldsymbol{D} &= [\underbrace{\boldsymbol{d}_1, \ldots, \boldsymbol{d}_{N_\mathrm{t}(K+L-1)}}_{\boldsymbol{D}_\mathrm{x}}, \underbrace{\boldsymbol{d}_{N_\mathrm{t}(K+L-1)+1}, \ldots, \boldsymbol{d}_{N_\mathrm{r}K}}_{\boldsymbol{D}_\mathrm{w}}] \\ &= [\boldsymbol{D}_\mathrm{x}, \boldsymbol{D}_\mathrm{w}] \end{aligned} \quad (41)$$

where $\boldsymbol{D}_\mathrm{x}$ is the signal subspace and $\boldsymbol{D}_\mathrm{w}$ is the noise subspace. Using the principle of orthogonality of the signal space and the noise space, we obtain

$$\tilde{\boldsymbol{y}}(n) = \boldsymbol{D}^\dagger \boldsymbol{y}_K(n) \quad (42)$$

$$= \boldsymbol{D}^\dagger \bar{\boldsymbol{H}}\boldsymbol{x}_K(n) + \boldsymbol{D}^\dagger \boldsymbol{v}(n) \quad (43)$$

$$= \begin{bmatrix} \boldsymbol{D}_\mathrm{x}^\dagger \bar{\boldsymbol{H}}\boldsymbol{x}_K(n) + \boldsymbol{D}_\mathrm{x}^\dagger \boldsymbol{v}(n) \\ \boldsymbol{D}_\mathrm{w}^\dagger \boldsymbol{v}(n) \end{bmatrix}. \quad (44)$$

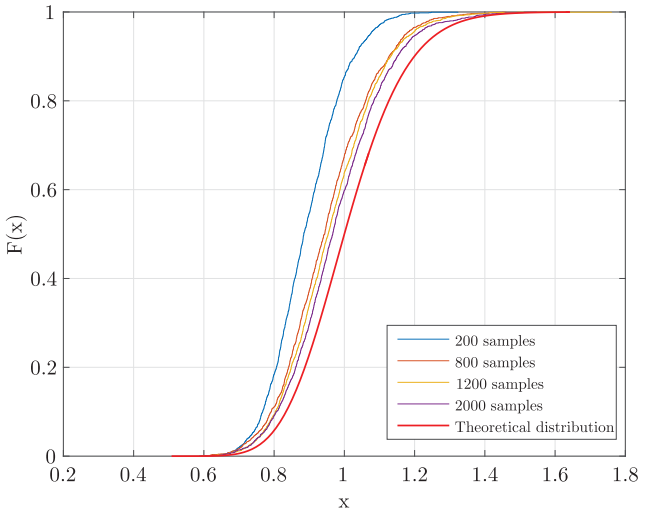

FIGURE 3. Empirical cumulative distribution and theoretical cumulative distribution of the test statistic T_q with 200, 800, 1200, and 2000 samples.

We can see from (44) that $\tilde{\boldsymbol{y}}$ is divided into two parts: the first part consists of the signal and the noise while the second part only contains the noise. We assume that there are κ noise components, $\kappa = 2, 3, \ldots, N_\mathrm{r}$. Take a noise samples for the $(q-1)$th noise component and take b noise samples for the qth noise component, $q = 2, 3, \ldots, \kappa$. Then, we have

$$\frac{\sum_{n=1}^{a} |\tilde{y}_{q-1}(n)|^2}{\sigma^2} \sim \chi^2(a) \quad (45)$$

$$\frac{\sum_{n=1}^{b} |\tilde{y}_{q}(n)|^2}{\sigma^2} \sim \chi^2(b) \quad (46)$$

$$\frac{\sum_{n=1}^{a} |\tilde{y}_{q-1}(n)|^2}{\sum_{n=1}^{b} |\tilde{y}_{q}(n)|^2} \sim F(a,b). \quad (47)$$

Let

$$T_q = \frac{\sum_{n=1}^{a} |\tilde{y}_{q-1}(n)|^2}{\sum_{n=1}^{b} |\tilde{y}_{q}(n)|^2} \quad (48)$$

where T_q is the test statistic, which does not require the prior knowledge of the noise power. In practice, we can only obtain the sample covariance matrix with finite sample sizes. To demonstrate the validity of the constructed T_q, the empirical cumulative distribution function (CDF) of T_q and the theoretical CDF are plotted in Fig. 3 for the different sample sizes. As shown in Fig. 3, when the number of samples increases, the distribution of the test statistic T_q approaches the theoretical distribution, which illustrates that T_q is reasonable and has a strong reliability even when the number of samples is finite. $N_\mathrm{t}(K+L-1)$ is then determined through a series of binary hypothesis tests. The decision criterion is represented as

$$T_q < T_\alpha, \quad \text{under } \mathcal{H}_0 \quad (49)$$

$$T_q \geq T_\alpha, \quad \text{under } \mathcal{H}_1 \quad (50)$$

where the hypothesis $\mathcal{H}_0$ represents the qth component belongs to the signal subspace and the hypothesis $\mathcal{H}_1$ denotes

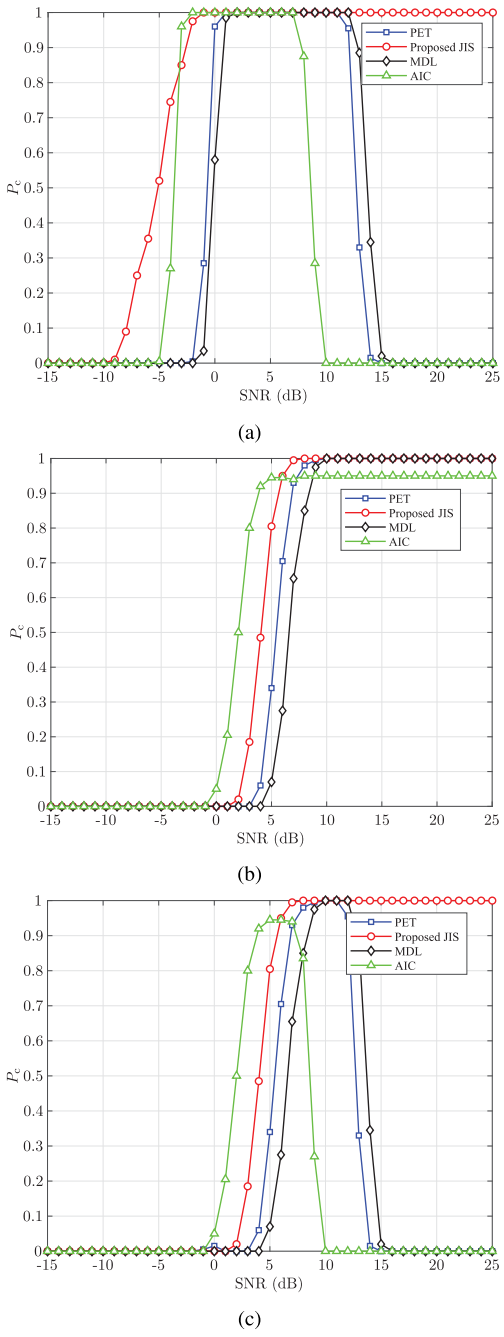

FIGURE 4. Identification performance comparison for the proposed joint identification scheme (JIS), the conventional Akaike information criterion (AIC) [16], the minimum description length (MDL) [16], and the predicted eigenvalue threshold (PET) [20]: (a) number of transmit antennas N_t, (b) expression $N_t(K+L-1)$, and (c) channel order L.

the qth component belongs to the noise subspace. The threshold T_α based on the miss probability is set as

$$P(F(a,b) < T_\alpha | \mathcal{H}_1) = \alpha \tag{51}$$

where α is the miss probability. Finally, the channel order L is determined using the obtained number of transmit antennas in the frequency domain. The proposed identifier based on F distribution is summarized in Algorithm 2.

Algorithm 2 Identifier via F Distribution

Input: $\boldsymbol{y}$ and $\hat{N}_t$;

1: Initialize $\kappa = 2$, α, a, b, and K;
2: Compute T_α using (51);
3: Compute the signal and noise subspace using (43);
4: Let $q = \kappa$ and calculate T_q using (48);
5: If $T_q \geq T_\alpha$, let $\kappa = \kappa + 1$, and repeat step 4 and 5; Otherwise, stop test;
6: Compute the channel order $L = \frac{N_r K - \kappa + 1}{\hat{N}_t} - K + 1$.

Remark 1: It is important to highlight that our scheme can identify the number of the transmit antennas and the channel order without the prior knowledge of noise power. Specifically, the signal subspace is explored to determine the number of transmit antennas using the proposed weighted Gerschgorin disk identifier, in which the only input to the identifier is the received signal, as shown in Algorithm 1. Furthermore, we design a test statistic based on F distribution to determine the channel order. Different from the traditional chi-square distribution, F distribution is used by dividing two chi-square distributions. Thus, the proposed identifier via F distribution does not require the prior knowledge of noise power, as shown in Algorithm 2.

C. ASYMPTOTIC CONSISTENCY

Theorem 1: The identifier via F distribution is asymptotically consistent when $a = b = N_s$, i.e.

$$\lim_{N_s \to \infty} P(\hat{\tau} = N_t(K+L-1) | a = b = N_s) = 1 \tag{52}$$

where $\hat{\tau}$ is the estimated value of $N_t(K+L-1)$.

Proof: When $N_s = a = b \to \infty$, then $F(a,b) = F(\infty,\infty) = 1$, thus we obtain

$$\lim_{N_s \to \infty} T_\alpha = 1. \tag{53}$$

Under the hypothesis $\mathcal{H}_0$, we have $N_r K - N_t(K+L-1) + 1 \leq q \leq N_r$. Let $q = N_r K - N_t(K+L-1) + 1$, we get

$$\lim_{N_s \to \infty} T_q = \lim_{N_s \to \infty} \frac{\sum_{n=1}^{N_s} |\tilde{y}_{q-1}(n)|^2}{\sum_{n=1}^{N_s} |\tilde{y}_q(n)|^2} < 1 \tag{54}$$

Thus,

$$\lim_{N_s \to \infty} P(T_q < T_\alpha | \mathcal{H}_0) = 1. \tag{55}$$

Under the hypothesis $\mathcal{H}_1$, we have $2 \leq q \leq N_r K - N_t(K+L-1)$, then

$$\lim_{N_s \to \infty} T_q = \lim_{N_s \to \infty} \frac{\sum_{n=1}^{N_s} |\tilde{y}_{q-1}(n)|^2}{\sum_{n=1}^{N_s} |\tilde{y}_q(n)|^2} = 1 \tag{56}$$

so,

$$\lim_{N_s \to \infty} P(T_q = T_\alpha | \mathcal{H}_1) = 1. \tag{57}$$

According to (55) and (57), we obtain

$$\lim_{N_s\to\infty} P(\hat{\tau} = N_t(K+L-1)|a=b=N_s) = 1. \quad (58)$$

□

V. SIMULATION RESULTS

In this section, we first describe the simulation parameters. Then, we compare the identification performance of the proposed approaches with the AIC, the MDL and the PET algorithms in [16] and [20]. Finally, we evaluate the robustness of the proposed identifier to the number of transmit antennas, and the number of the channel paths, and the identification error. The probability of the correct identification, denoted by P_c, is used as the metric of the identification performance.

A. SIMULATION SETUP

The transmitted data is modulated as quadrature phase-shift-keying (QPSK) symbols with the spatial multiplexing transmission scheme. The length of FFT is set to 64 and the size of the cyclic prefix is 10. The number of OFDM symbol in a block is 100. The miss probability is set to 0.015. The performance metric is obtained based on 2000 Monte Carlo trials.

B. PERFORMANCE ANALYSIS

Fig. 4 illustrates the identification performance of the proposed schemes, along with the existing methods in [16] and [20] with $N_r = 15$, $L = 4$, $N_t = 5$, and $K = 4$. To ensure fairness, all methods are evaluated using the same domain of the received signal. In other words, the number of transmit antennas is identified using the frequency domain signal, whereas the channel order is obtained using the time domain signal. It is clear that the proposed joint identification scheme (JIS) achieves a high identification accuracy for both the number of transmit antennas and the channel order even at a relatively low SNR and a very high SNR. Specifically, we observe from Fig. 4(a) that the improved weighted Gerschgorin disk identifier in the joint identification scheme obtains the best identification performance among the existing methods over all the SNRs. Our improved weighted Gerschgorin disk identifier can achieve the identification accuracy $P_c = 1$ when SNR > -3 dB whereas the traditional methods cannot work when SNR > 15 dB. Note that the weighted Gerschgorin disk identifier in [32] fails over all SNR and thus is not shown in the figure. Fig. 4(b) shows the identification performance for $N_t(K+L-1)$. We can see that the proposed identifier via F distribution in the joint identification scheme outperforms the MDL and the PET methods over all SNRs. Although the proposed identifier does not perform as well as the AIC method at a low SNR, the identification accuracy of the AIC method cannot reach 1 in a high SNR. In Fig. 4(c), the identification accuracy of the channel order is evaluated. It can be seen from Fig. 4(c) that, the probability of the correct

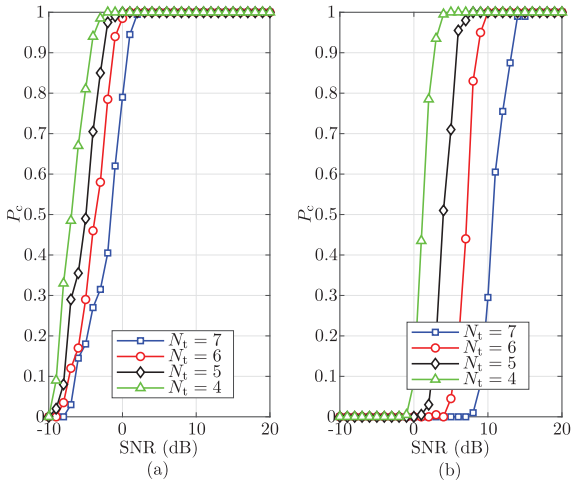

FIGURE 5. Correct identification probability evaluation for the proposed joint identification scheme (JIS) in cases of different numbers of transmit antennas: (a) number of transmit antennas N_t, and (b) channel order L.

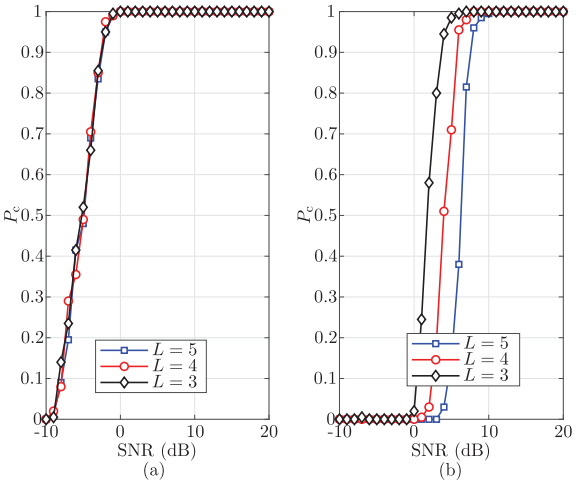

FIGURE 6. Correct identification probability evaluation for the proposed joint identification scheme (JIS) in cases of different channel orders: (a) number of transmit antennas N_t, and (b) channel order L.

identification of the proposed joint identification scheme reaches 1 while the existing methods in [16] and [20] all fail at a high SNR. This is because the rank of the covariance matrix of the received signal increases under the multiple transmit antennas and the multiple channel paths in the MIMO-OFDM system. Thus, these results demonstrate that the proposed scheme can effectively detect the number of transmit antennas and the channel order simultaneously in the MIMO-OFDM system. Regarding the computational load, the complexity of our scheme mainly comes from EVD, which is similar to conventional algorithms such as AIC [16], MDL [16], and PET [20]. In our work, the quadrature right-triangle (QR) algorithm is used in the EVD. Thus, the computational complexity of the estimation of N_t and L is order of $\mathcal{O}(N_r^3)$ and $\mathcal{O}(K^3N_r^3)$, respectively. This means that our method has the same low complexity as the conventional algorithms.

Fig. 5 shows the identification performance of the proposed scheme with different numbers of transmit antennas. As expected, the identification performance of the number

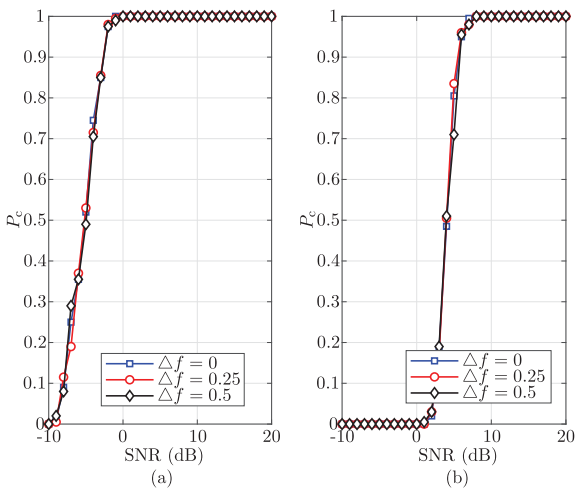

FIGURE 7. Correct identification probability evaluation for the proposed joint identification scheme (JIS) in cases of different normalized frequency offsets: (a) number of transmit antennas N_t, and (b) channel order L.

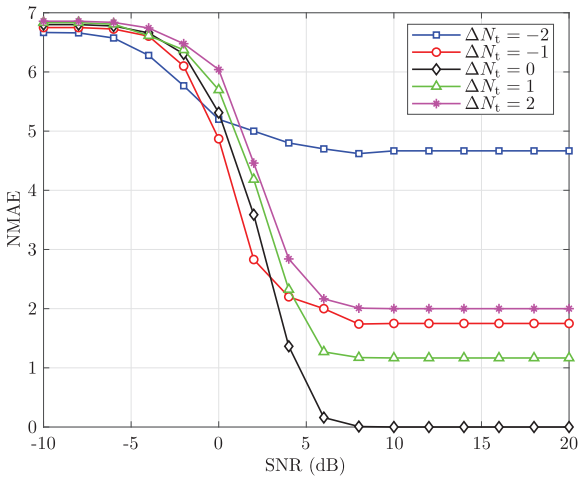

FIGURE 8. Normalized mean absolute error evaluation of the channel order for the proposed joint identification scheme (JIS) in cases of different identification errors of the number of transmit antennas.

of transmit antennas and the channel order decreases as the number of transmit antennas increases. This is because an increase in the number of antennas leads to a reduction in the noise subspace. In Fig. 6, the identification performance of the proposed scheme with different channel orders is evaluated. Encouragingly, increasing the channel order has little effect on the identification accuracy of the number of transmit antennas. This result indicates that the improved weighted Gerschgorin disk identifier is robust to the channel order. This is because the well-designed diagonal matrix based on the second moment of the circle center and an adaptive threshold can combat the error term caused by multiple channel paths. However, the identification performance of the channel order degrades as the channel order increases. Fig. 7 shows the identification performance of the proposed scheme with different frequency offsets. We can see that, the identification performance of our scheme does not vary as the frequency offset, which means that the proposed scheme is robust to the frequency offset. Fig. 8 shows the normalized mean absolute error (NMAE) of the channel order with different identification errors of the number of transmit antennas. It can be seen that, as the identification error of the number of transmit antennas increases, the NMAE of the channel order increases. Furthermore, we note that the underestimation leads to a larger NMAE of the channel order than the overestimation of the number of transmit antennas.

VI. CONCLUSION

In this paper, a novel joint identification scheme of the number of transmit antennas and the channel order was proposed for the MIMO-OFDM system, which can address the coupling effect. The proposed joint scheme exploited the time and frequency domains of the received signal. First, an improved weighted Gerschgorin disk identifier was designed to detect the number of transmit antennas using the frequency domain signal. The equivalent time-domain model for the MIMO-OFDM system was then derived to improve the utilization of the receiver antennas. Furthermore, a novel identifier based on F distribution was proposed to estimate $N_t(K + L - 1)$. Finally, the channel order was determined using the number of transmit antennas obtained in the frequency domain. Extensive simulation results showed that the proposed scheme exhibits the excellent performance and outperforms existing approaches. Since the proposed scheme can well combat the coupling effect due to the transmit antenna and the multiple channel paths, it is expected to be widely used in practical MIMO-OFDM systems.

REFERENCES

[1] M. Kulin, T. Kazaz, I. Moerman, and E. De Poorter, "End-to-end learning from spectrum data: A deep learning approach for wireless signal identification in spectrum monitoring applications," *IEEE Access*, vol. 6, pp. 18484–18501, 2018.

[2] K. Kim, C. M. Spooner, I. Akbar, and J. H. Reed, "Specific emitter identification for cognitive radio with application to IEEE 802.11," in *Proc. IEEE Global Telecommun. Conf. (GLOBECOM)*, Dec. 2008, pp. 1–5.

[3] A. Gorcin and H. Arslan, "Signal identification for adaptive spectrum hyperspace access in wireless communications systems," *IEEE Commun. Mag.*, vol. 52, no. 10, pp. 134–145, Oct. 2014.

[4] P. Zhang, T. Taleb, X. Jiang, and B. Wu, "Physical layer authentication for massive MIMO systems with hardware impairments," *IEEE Trans. Wireless Commun.*, vol. 19, no. 3, pp. 1563–1576, Mar. 2020.

[5] W. Hou, X. Wang, J.-Y. Chouinard, and A. Refaey, "Physical layer authentication for mobile systems with time-varying carrier frequency offsets," *IEEE Trans. Commun.*, vol. 62, no. 5, pp. 1658–1667, May 2014.

[6] K. Merchant, S. Revay, G. Stantchev, and B. Nousain, "Deep learning for RF device fingerprinting in cognitive communication networks," *IEEE J. Sel. Topics Signal Process.*, vol. 12, no. 1, pp. 160–167, Feb. 2018.

[7] D. Yang, W. Zhang, Q. Ye, C. Zhang, N. Zhang, C. Huang, H. Zhang, and X. Shen, "DetFed: Dynamic resource scheduling for deterministic federated learning over time-sensitive networks," *IEEE Trans. Mobile Comput.*, early access, 2023, doi: 10.1109/TMC.2023.3303017.

[8] W. Zhang, D. Yang, W. Wu, H. Peng, N. Zhang, H. Zhang, and X. Shen, "Optimizing federated learning in distributed industrial IoT: A multi-agent approach," *IEEE J. Sel. Areas Commun.*, vol. 39, no. 12, pp. 3688–3703, Dec. 2021.

[9] B. He and F. Wang, "Cooperative specific emitter identification via multiple distorted receivers," *IEEE Trans. Inf. Forensics Security*, vol. 15, pp. 3791–3806, Jun. 2020.

[10] Y. A. Eldemerdash, O. A. Dobre, and M. Öner, "Signal identification for multiple-antenna wireless systems: Achievements and challenges," *IEEE Commun. Surveys Tuts.*, vol. 18, no. 3, pp. 1524–1551, 3rd Quart., 2016.
[11] M. Gao, Y. Li, O. A. Dobre, and N. Al-Dhahir, "Blind identification of SFBC-OFDM signals based on the central limit theorem," *IEEE Trans. Wireless Commun.*, vol. 18, no. 7, pp. 3500–3514, Jul. 2019.
[12] M. Marey, O. A. Dobre, and B. Liao, "Classification of STBC systems over frequency-selective channels," *IEEE Trans. Veh. Technol.*, vol. 64, no. 5, pp. 2159–2164, May 2015.
[13] M. Marey and O. A. Dobre, "Blind modulation classification algorithm for single and multiple-antenna systems over frequency-selective channels," *IEEE Signal Process. Lett.*, vol. 21, no. 9, pp. 1098–1102, Sep. 2014.
[14] Y. A. Eldemerdash, O. A. Dobre, and B. J. Liao, "Blind identification of SM and Alamouti STBC-OFDM signals," *IEEE Trans. Wireless Commun.*, vol. 14, no. 2, pp. 972–982, Feb. 2015.
[15] Y. Liu, O. Simeone, A. M. Haimovich, and W. Su, "Modulation classification for MIMO-OFDM signals via Gibbs sampling," in *Proc. 49th Annu. Conf. Inf. Sci. Syst. (CISS)*, Mar. 2015, pp. 1–6.
[16] O. Somekh, O. Simeone, Y. Bar-Ness, and W. Su, "Detecting the number of transmit antennas with unauthorized or cognitive receivers in MIMO systems," in *Proc. IEEE Mil. Commun. Conf. (MILCOM)*, Oct. 2007, pp. 1–5.
[17] K. Hassan, C. N. Nzéza, R. Gautier, E. Radoi, M. Berbineau, and I. Dayoub, "Blind detection of the number of transmitting antennas for spatially-correlated MIMO systems," in *Proc. 11th Int. Conf. ITS Telecommun.*, Aug. 2011, pp. 458–462.
[18] M.-R. Oularbi, S. Gazor, A. Aissa-El-Bey, and S. Houcke, "Enumeration of base station antennas in a cognitive receiver by exploiting pilot patterns," *IEEE Commun. Lett.*, vol. 17, no. 1, pp. 8–11, Jan. 2013.
[19] M. Mohammadkarimi, E. Karami, O. A. Dobre, and M. Z. Win, "Number of transmit antennas detection using time-diversity of the fading channel," *IEEE Trans. Signal Process.*, vol. 65, no. 15, pp. 4031–4046, Aug. 2017.
[20] W. Chen, K. M. Wong, and J. P. Reilly, "Detection of the number of signals: A predicted eigen-threshold approach," *IEEE Trans. Signal Process.*, vol. 39, no. 5, pp. 1088–1098, May 1991.
[21] T. Li, Y. Li, L. J. Cimini, and H. Zhang, "Hypothesis testing based fast-converged blind estimation of transmit-antenna number for MIMO systems," *IEEE Trans. Veh. Technol.*, vol. 67, no. 6, pp. 5084–5095, Jun. 2018.
[22] T. Li, Y. Li, Y. Chen, L. J. Cimini, and H. Zhang, "Estimation of MIMO transmit-antenna number using higher-order moments-based hypothesis testing," *IEEE Wireless Commun. Lett.*, vol. 7, no. 2, pp. 258–261, Apr. 2018.
[23] T. Li, Y. Li, L. J. Cimini, and H. Zhang, "Blind estimation of transmit-antenna number for non-cooperative multiple-input multiple-output orthogonal frequency division multiplexing systems," *IET Commun.*, vol. 11, no. 17, pp. 2637–2642, Nov. 2017.
[24] J. Vijayamohanan, A. Gupta, O. Noakoasteen, S. K. Goudos, and C. G. Christodoulou, "Source detection with multi-label classification," *IEEE Open J. Signal Process.*, vol. 4, pp. 336–345, 2023.
[25] M. Gao, Y. Li, O. A. Dobre, and N. Al-Dhahir, "Joint blind identification of the number of transmit antennas and MIMO schemes using Gerschgorin radii and FNN," *IEEE Trans. Wireless Commun.*, vol. 18, no. 1, pp. 373–387, Jan. 2019.
[26] M. Chen, Y.-H. Xiao, Q. Li, L. Feng, M. Rihan, and N. Guo, "One-bit source number detection via neural network," in *Proc. 5th Int. Conf. Inf. Commun. Signal Process. (ICICSP)*, Shenzhen, China, Nov. 2022, pp. 91–95.
[27] S. Zhou, T. Li, Y. Li, R. Zhang, and Y. Ruan, "Source number estimation via machine learning based on eigenvalue preprocessing," *IEEE Commun. Lett.*, vol. 26, no. 10, pp. 2360–2364, Oct. 2022.
[28] D. T. Hoang and K. Lee, "Coherent signal enumeration based on deep learning and the FTMR algorithm," in *Proc. IEEE Int. Conf. Commun. (ICC)*, May 2022, pp. 5098–5103.
[29] L. T. Thanh, K. Abed-Meraim, and N. L. Trung, "Misspecified Cramér–Rao bounds for blind channel estimation under channel order misspecification," *IEEE Trans. Signal Process.*, vol. 69, pp. 5372–5385, 2021.
[30] M. Wax and A. Adler, "FIR-SIMO channel order determination by invariant-signal-subspace matching," *Digit. Signal Process.*, vol. 134, Apr. 2023, Art. no. 103914.
[31] Y. Wang and L. Jin, "Blind order estimation based on subspace identification and weighted least squares equalization," in *Proc. IEEE 81st Veh. Technol. Conf. (VTC Spring)*, May 2015, pp. 1–5.
[32] F. Samsami Khodadad and G. Abed Hodtani, "Blind joint estimation of channel order and the number of active users in direct sequence code-division multiple-access multi-path channels," *IET Signal Process.*, vol. 8, no. 2, pp. 158–166, Apr. 2014.
[33] J. Tian, T. Zhou, T. Xu, H. Hu, and M. Li, "Blind estimation of channel order and SNR for OFDM systems," *IEEE Access*, vol. 6, pp. 12656–12664, 2018.
[34] H.-R. Park, "Adaptive channel estimation for OFDM systems using CIR length estimate," *IEEE Wireless Commun. Lett.*, vol. 10, no. 11, pp. 2597–2601, Nov. 2021.
[35] H.-R. Park, "A low-complexity channel estimation for OFDM systems based on CIR length adaptation," *IEEE Access*, vol. 10, pp. 85941–85951, 2022.
[36] K. A. Babu, U. Satija, B. Ramkumar, and M. S. Manikandan, "Blind channel length estimation for OFDM systems using cumulant features," in *Proc. Int. Symp. Wireless Pers. Multimedia Commun. (WPMC)*, Hyderabad, India, Dec. 2015, pp. 1–4.
[37] H.-T. Wu, J.-F. Yang, and F.-K. Chen, "Source number estimators using transformed Gerschgorin radii," *IEEE Trans. Signal Process.*, vol. 43, no. 6, pp. 1325–1333, Jun. 1995.

CHAO WANG received the M.A.Eng. degree from the School of Electronic Information Engineering, Beihang University, Beijing, China, in 2012. He is currently a Senior Engineer with China Academy of Space Technology. His research interests include spaceborne information processing, satellite communication, and signal processing.

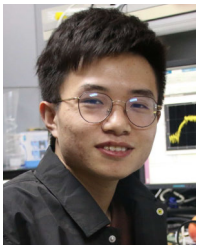

BOXIANG HE received the B.Eng. degree from the School of Electronic and Information Engineering, Beijing Jiaotong University, Beijing, China, in 2018, where he is currently pursuing the Ph.D. degree with the State Key Laboratory of Advanced Rail Autonomous Operation, Frontiers Science Center for Smart High-Speed Railway System, School of Electronic and Information Engineering, Beijing Jiaotong University. His current research interests include signal identification, physical layer security, integrated sensing and communication, and signal processing.

FANGGANG WANG (Senior Member, IEEE) received the B.Eng. and Ph.D. degrees from the School of Information and Communication Engineering, Beijing University of Posts and Telecommunications, Beijing, China, in 2005 and 2010, respectively. He was a Postdoctoral Fellow with the Institute of Network Coding, The Chinese University of Hong Kong, Hong Kong, from 2010 to 2012. He was a Visiting Scholar with the Massachusetts Institute of Technology, from 2015 to 2016, and the Singapore University of Technology and Design, in 2014. He is currently a Professor with the State Key Laboratory of Advanced Rail Autonomous Operation, Frontiers Science Center for Smart High-Speed Railway System, School of Electronic and Information Engineering, Beijing Jiaotong University. His research interests include wireless communications, signal processing, and information theory. He served as an Editor for IEEE COMMUNICATIONS LETTERS and a technical program committee member for several conferences.